

Formation of D inventories and structural modifications by deuterium bombardment of tungsten thin films

I. Bizyukov^{a,b,*}, K. Krieger^a, N. Azarenkov^b, S. Levchuk^a, Ch. Linsmeier^a

^a *Max-Planck-Institut für Plasmaphysik, EURATOM Association, Boltzmannstraße 2, D-85748 Garching, Germany*

^b *Kharkiv National University, Faculty of Physics and Technologies, 31 Kurchatov Ave., Kharkiv 61108, Ukraine*

Abstract

Magnetron deposited W layers were irradiated with 9 keV D₃⁺ ions up to fluences of 7×10^{23} D/m². The erosion of the tungsten layers and the formation of D inventories were investigated by means of ion beam analysis. Under certain conditions blistering of the W-layer was observed. The measured W sputtering yield and deuterium depth distribution are compared with those measured for bulk tungsten. The results show that W films are a suitable alternative to bulk tungsten in experiments on plasma-wall interactions with significantly improved diagnostic accessibility.

© 2004 Elsevier B.V. All rights reserved.

PACS: 79.20.Rf

Keywords: Ion-surface interactions; Deuterium inventory; Tungsten; Sputtering; Retention

1. Introduction

In nearly all design studies of future nuclear fusion devices, tungsten is foreseen as plasma-facing material at least in the divertor region [1]. Apart from its high energy threshold for sputtering, tungsten does not suffer from chemical sputtering as carbon does. Furthermore, tritium does not co-deposit with tungsten [2], which avoids the potentially serious radioactive inventory problem as in the case of carbon. Tungsten sputtered at divertor and baffle surfaces by the high-flux bombardment with hydrogen and impurity atoms and ions is partly redeposited non-locally due to migration processes [3]. Thus, tungsten layers will develop on parts

of the plasma-facing surfaces whose properties may differ from the properties of polycrystalline and crystalline tungsten in terms of erosion, hydrogen isotope retention and diffusion into the bulk material.

In contrast to bulk material, erosion of W films can be investigated not only by weight loss measurements but also using Rutherford backscattering (RBS) and nuclear reaction analysis (NRA). These ion beam techniques also provide information on the depth distribution of incident species and target atoms, which is essential for the investigation of processes like co-bombardment of fuel atoms with impurities, film growth and diffusion of incident particles. Apart from their relevance for re-deposited W layers in fusion devices, W films provide an attractive alternative to bulk tungsten in particular for experiments on co-bombardment of W with D and various impurity ions. For these studies it is essential to note that the relevant physical properties of the W films are similar to those of bulk tungsten.

* Corresponding author. Tel.: +49 89 3299 1846; fax: +49 89 3299 2279.

E-mail addresses: ivan.bizyukov@ipp.mpg.de (I. Bizyukov), krieger@ipp.mpg.de (K. Krieger).

2. Experimental

2.1. Preparation and characterisation of samples

Tungsten layers were prepared on a carbon substrate with an intermediate Cu layer. The substrate consisted of polished pyrolytic graphite with dimensions $10 \times 15 \times 0.525$ mm. This sample structure has the following advantages:

- The adhesive properties of copper result in a well defined Cu/W interface with a sharp transition between the two materials, providing a good depth resolution of the RBS analysis.
- The Cu and W parts of the RBS spectrum appear separated from each other, facilitating quantitative determination of the W and Cu area densities.
- Cu prevents diffusion of hydrogen isotopes into the substrate material, which facilitates determination of D depth profiles.
- Cu does not form carbides and does not form an alloy with W. Furthermore the melting temperature of Cu is high enough to allow annealing at temperatures of up to 800 °C after film deposition, which is required to decrease mechanical stresses while still maintaining a stable boundary between the W and the Cu layer.

The metal films were deposited using magnetron sputtering with argon as working gas. To minimise the contamination of the deposited films with oxygen, the residual pressure was maintained at values of $\approx 10^{-7}$ mbar using a turbo-molecular pump and a liquid nitrogen cooling trap. Before deposition the sample surface was cleaned by Ar sputtering. Then the Cu and W layers were deposited one after another in the same process.

The films were characterized by X-ray photoelectron spectroscopy (XPS), Rutherford back-scattering spectroscopy (RBS) and scanning electron microscopy (SEM). The W and Cu area density of the layers was determined for each sample by analysis of RBS spectra using the SIMNRA program [4]. The area density of the W layer was determined to be 1.44×10^{22} W/m² which, assuming bulk tungsten density, corresponds to a thickness of 200 nm; for the Cu layer the corresponding values are 3.4×10^{22} Cu/m² and 400 nm, respectively. The data for different samples scatter by up to 3% depending on the sample's location during the deposition process. Concentrations of light impurities were determined by XPS analysis. For carbon one obtains an upper limit of 0.5%, for nitrogen 0.5% and for oxygen 0.7%. The atomic densities of the W and Cu layers were calculated by combining SEM and RBS measurements with an estimated experimental error of 10%. For the SEM images the error originates mainly from the limited

accuracy in the determination of the exact position of the layer interface, while for RBS the main error source is the measurement of the accumulated ion beam charge. Within these experimental errors the layer densities were found to agree with the densities of the bulk materials. The depth distribution of both layer materials was also measured before and after the annealing procedure. Comparison of both measurements shows that the transition between the W and Cu layers remains stable and therefore allows to extend the experiments to high temperatures.

2.2. Setup of the irradiation experiment

The experimental setup used for the irradiation of the W samples consists of a vacuum chamber, and an attached duoplasmatron ion beam system with a 60° mass analysing magnet, which is deflecting the beam into a high energy ion beam line connecting a Tandem accelerator to the target chamber. For ion beam analysis (IBA) the analyzing magnet is switched off to pass the high energy beam to the target. The setup with irradiation beam and analysis beam passing the same aperture system ensures perfect overlap of irradiation and analysis spots on the samples.

For ion beam analysis the target chamber is equipped with two high resolution solid state particle detectors at scattering angles of 165° and 105° and an additional detector covering a large solid angle for detection of protons from nuclear reactions. The target is mounted inside a Faraday cup to ensure accurate measurement of the beam current. The residual pressure in the vacuum chamber during analysis is $< 5 \times 10^{-7}$ mbar and during bombardment $< 2 \times 10^{-6}$ mbar. For the experiments discussed here, the temperature of the samples remained steady at room temperature.

The beam defining aperture has a diameter of 2 mm and is installed at a distance to the target of 15 mm. The corresponding beam spot on the target is the exact image of the aperture because on this length scale the beam divergence is negligible. Irradiation of a-C:H films was used to determine the beam profile using optical microscopy and profilometry. The obtained actual diameter of the spot that can be used for conversion of the total D_3^+ ion beam current into the particle flux in the region of uniform irradiation is 1.8 mm. Accordingly, the 7 μ A current of the D_3^+ ions with an energy of 9 keV and an energy spread less than 25 eV used in the irradiation experiments corresponded to a flux of 5×10^{19} D/m². The error in the fluence measurement is <10% and is attributed mainly to deviations of the beam current from circular symmetry in the irradiation spot.

To avoid distortion of the ion beam analysis by measuring in the non-uniform edge region of the irradiation spots, the beam defining aperture can be exchanged in situ against one with a smaller diameter of 1 mm. The

misalignment of the analysis beam spot relatively to the irradiation beam spot was again determined by analysis of irradiated a-C:H films and is smaller than 0.2 mm. Consequently, only the uniformly irradiated region of the target is analyzed by IBA, and therefore, only depth variations of the elemental concentrations need to be considered in contrast to weight loss measurements where lateral variations of the irradiation current density can lead to significant errors.

2.3. Tungsten film irradiation experiments

In two sets of irradiation experiments W layers were irradiated step-by-step and initially and after each step the layers were analysed by RBS to measure the thickness of the tungsten film and by NRA using the reaction $D(^3\text{He}, ^4\text{He})p$ to determine the depth profile and total amount of implanted deuterium. The total amount of D in the W layers was obtained by comparing the integrated number of protons detected from the reaction $D(^3\text{He}, ^4\text{He})p$ to that of a-C:D film samples with known D content.

In a first series of experiments only the erosion of the W layer was studied by measuring the decreasing thickness of the W layer using RBS with ^4He ions. In the second series the D retention in the W layers was analysed in addition to the W erosion for irradiation fluences of up to $7.4 \times 10^{23} \text{ D/m}^2$.

3. Results and discussion

3.1. Sputtering yield

To determine the sputtering yield of a material by measurement of the erosion of a thin layer by ion beam analysis, it is of primary importance to minimise the experimental error of the irradiation fluence. By choosing the beam energy of the ^4He ions for RBS analysis appropriately it is possible to obtain spectra where the spectral parts for each element do not overlap. For the analysis of the RBS spectra, SIMNRA version 5.4 was used [4]. The uncertainty of the tabulated stopping powers used by the code introduces a systematic error, which, however, cancels out because only differences from the initial film thickness are relevant. This allows the absolute amount of sputtered W atoms to be determined within an error of $\pm 10^{20} \text{ W/m}^2$. Thus, the experimental error of the sputtering yield is defined by the accuracy of the irradiation fluence measurement, which is smaller than 10%. In the second set of irradiation experiments where 800 keV ^3He ions were used for optimized measurements of the D concentration, the W and Cu RBS peaks, which were simultaneously detected, overlap with consequently enlarged errors in determining the W layer thickness.

Fig. 1 shows the amount of sputtered W atoms as a function of D irradiation fluence. The W erosion yield was determined by a Bayesian straight line fit, which takes into account errors in both the independent and dependent variable. The small constant shift is due to an oxidized layer with a 15% oxygen fraction and a thickness of 28 nm, which covered the surface initially and disappeared after an irradiation fluence of $2.5 \times 10^{22} \text{ D/m}^2$. The resulting value of the W sputtering yield is $Y = 9.8 \times 10^{-3}$. Fig. 2 shows a set of W RBS peaks after subsequent irradiation steps during the first set of experiments. The low energy edge of the W peak keeps the same shape until the fluence reaches a value of $2.2 \times 10^{23} \text{ D/m}^2$ where blisters start to grow. This shows that during irradiation the D_3^+ ion beam profile keeps its shape and uniformity across the analysed area of the irradiation spot. Nonuniform irradiation would lead to nonuniform erosion, which in turn would lead to a shallower slope of the low energy edge of the W peak.

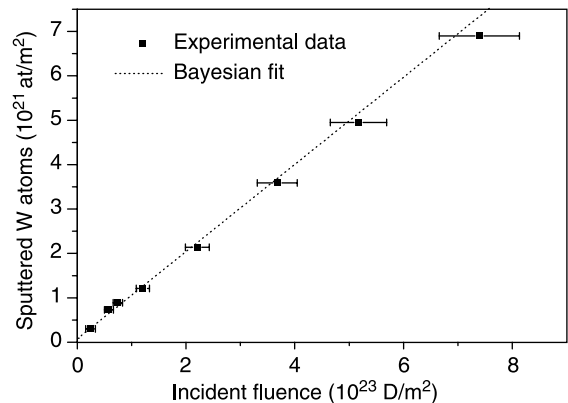


Fig. 1. Amount of sputtered W atoms per m^2 as a function of D irradiation fluence. The dotted line represents a Bayesian straight line fit.

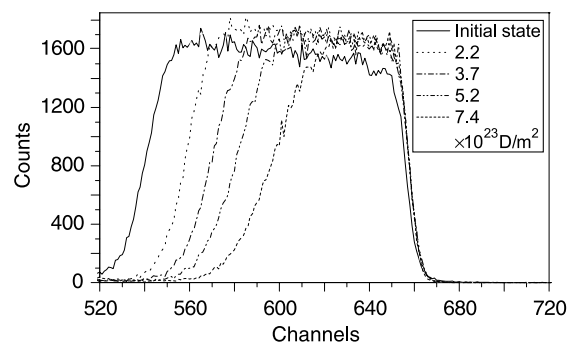


Fig. 2. RBS spectra during sequential irradiation of the W layer. The decrease of the slope of the low energy edge corresponds to the formation of blisters at the W/Cu interface.

The obtained sputtering yield was compared with theoretical and experimental data published in [5]. The experimental data in this publication were obtained by weight loss measurements for polycrystalline W ($Y \approx 5.2 \times 10^{-3}$) and the theoretical data were calculated with TRIM.SP [6] ($Y \approx 10 \times 10^{-3}$). The difference between the experimental results can be explained by the principally different measurement methods for the amount of sputtered particles. In the weight loss measurements in [5] the experimental error for the number of sputtered W atoms is about 40 times higher ($\pm 1 \mu\text{g}$) than the error in the RBS results presented here. The sputtering yield obtained from the film erosion measurements is in good agreement with the TRIM.SP results.

3.2. W layer blistering

In the RBS spectra shown in Fig. 2, the sharp transition at the low energy edge of the W signal smoothes out for incident fluences $> 2.2 \times 10^{23} \text{ D/m}^2$. Above this fluence, the transition from tungsten to copper at the W layer interface becomes increasingly shallow. This phenomenon is explained by the formation and growth of blisters with a diameter from 5 to 50 μm on the surface. SEM investigations show that the blisters are bubbles at the W/Cu interface resulting from detachment of the W layer. To clarify the nature of the bubbles, non-annealed W–Cu films were irradiated at the same conditions as annealed ones. In this case even at incident fluences well below $2 \times 10^{22} \text{ D/m}^2$ bubbles covered the main part of the irradiating spot. From these observations one can infer that the bubble formation is a result of mechanical stress. By annealing, the initially high stresses can be decreased sufficiently to prevent bubble formation in the range of fluences accessible to the described experimental setup.

3.3. D retention

The second campaign was devoted to the investigation of D retention in the W layer. The surface concentration of D retained in the W layer has been calculated according to the formula:

$$(Nt)_{\text{D}} = (Nt)_{\text{a-C:D}} \cdot \frac{I}{I_{\text{a-C:D}}} \cdot \frac{C_{\text{a-C:D}}}{C} \quad (1)$$

and the average atomic concentration of D retained has been calculated as

$$C_{\text{D:W}} = \frac{(Nt)_{\text{D}}}{(Nt)_{\text{W}} + (Nt)_{\text{D}}}, \quad (2)$$

where $(Nt)_{\text{D}}$ denotes the surface concentration of retained D, $(Nt)_{\text{a-C:D}}$ is the previously known surface concentration of D in a-C:D film calibration sample ($1.6 \times 10^{22} \text{ D/m}^2$), $(Nt)_{\text{W}}$ is the surface concentration of W, I is the area under the proton peak due to D retained

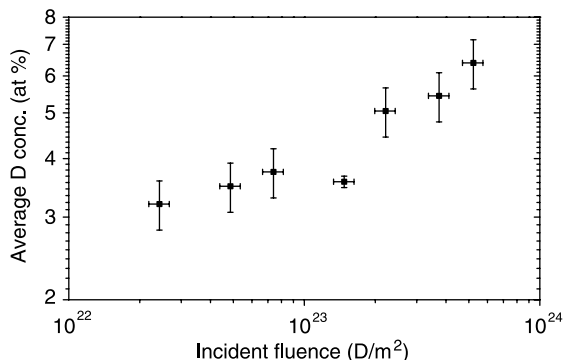


Fig. 3. Average D concentration in the W layer during sequential irradiation depending on incident fluence.

in the W layer, $I_{\text{a-C:D}}$ is the area under the proton peak of the a-C:D film, C is the collected charge during ion beam analysis of the W layer, $C_{\text{a-C:D}}$ is the collected charge during analysis of the a-C:D film calibration sample and $C_{\text{D:W}}$ is the atomic concentration of D retained in the W layer. Fig. 3 shows the thickness-averaged D concentration as a function of incident fluence. The relatively high initial D retention is caused by the thin oxidized layer on the surface. The small thickness of the W layer allows NRA to be performed in the whole depth range and to obtain the D depth profile as well as the average D atomic concentration in the layer.

After irradiation with a fluence of $1.5 \times 10^{23} \text{ D/m}^2$, the D depth profile was measured with a higher fluence ($66.3 \mu\text{C}$ in comparison with $5 \mu\text{C}$) of the analysing beam. The higher dose was necessary to reduce the statistical error in the α -particle spectrum of the $\text{D}(\text{}^3\text{He}, \alpha)\text{p}$ reaction (Fig. 4(a)), which is used for the derivation of the D depth profile. In this case, however, the beam-induced release of deuterium from the sample is no longer negligible as seen in Fig. 3. The α -spectrum shown in Fig. 4(a) was measured at a scattering angle of 105° . The obtained data were smoothed and the depth distribution of retained D was derived by fitting the spectrum with the SIMNRA program. Fig. 4(b) shows the resulting depth profile of the D atomic concentration in the W layer. The D concentration rises to $\approx 10\text{at.}\%$ just under the surface with the D rich zone extending to a depth of 70 nm, after which it decreases slowly towards the W/Cu interface. Although the total concentration fits well with the absolute amount of D derived from the integral proton peak at the corresponding irradiation fluence, the individual error of the concentration values is in the range of 40% to 60% due to the low spectral counts. Similar concentrations in the ion implanted zone were obtained in [7] by implanting 10 keV D ions into a single crystal W along the $\langle 111 \rangle$ direction up to a fluence of $4 \times 10^{22} \text{ D/m}^2$ and in [8,9] by implanting 1 keV D ions into polycrystalline W with a fluence of up to

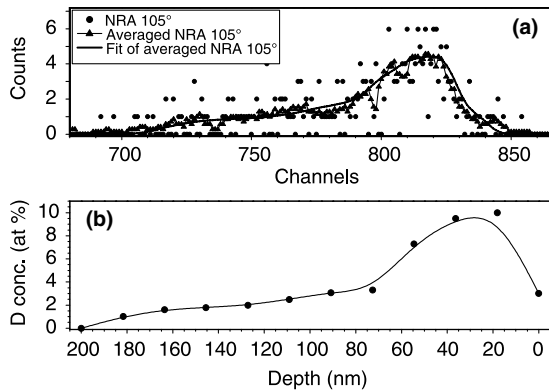


Fig. 4. (a) NRA α -spectrum at a scattering angle of 105° . The acquired NRA spectrum was smoothed and the D depth distribution was obtained by fitting the data with SIMNRA. (b) Resulting depth profile of the D atomic concentration.

10^{24} D/m². In [7] and [9] the same NRA reaction and in [8] elastic recoil detection was used for D depth profiling.

4. Conclusions

Magnetron sputtering deposited W films were characterised and irradiated with 9 keV D₃⁺ ions. The influence of the D irradiation on W layer erosion, mechanical stress levels and D inventories were investigated. The sputtering yield was found to be higher than that obtained for polycrystalline W in experiments based on weight loss measurements, but closer to theoretical values calculated by TRIM.SP. Mechanical stress results in blisters on the W layer surface, however, their formation can be avoided for up to one order of magnitude higher fluences by thermal annealing. In contrast, blistering of bulk W was only observed at fluences

$> 3 \times 10^{25}$ D/m² with energies ≥ 100 eV [10]. In brief, it can be concluded that W films provide a suitable replacement of bulk tungsten in experiments on plasma-wall interactions with significantly better diagnostic accessibility.

Acknowledgments

We would like to thank P. Matern, T. Dürbeck, B. Plöckl, J. Dorner and M. Fusseder for their technical assistance; G. Matern for SEM and optical microscopy; Drs U. von Toussaint, V. Alimov, W. Eckstein, R. Behrisch and J. Roth, for helpful discussions.

References

- [1] G. Janeschitz, ITER JCT and ITER HTs, *J. Nucl. Mater.* 1 (2001) 290.
- [2] H. Maier, K. Krieger, A. Tabasso, S. Lindig, V. Rohde, J. Roth. in: *Proceedings of the 26th European Conference on Plasma Phys. Control. Fus.*, 23J, Maastricht, ECA, 1999, p. 1509.
- [3] K. Krieger et al., *J. Nucl. Mater.* 313–316 (2003) 327.
- [4] M. Mayer, MPI f. Plasmaphysik, Technical report IPP 113 (9).
- [5] W. Eckstein et al., *Sputtering data*, IPP report 9/82, February 1993.
- [6] W. Eckstein, *Computer Simulation of Ion–Solid Interaction*, Springer, Berlin, 1991.
- [7] V.Kh. Alimov, K. Ertl, J. Roth, K. Schmid, *Phys. Scr. T* 94 (2001) 34.
- [8] W. Wang, J. Roth, S. Lindig, C.H. Wu, *J. Nucl. Mater.* 299 (2001) 124.
- [9] A.A. Haasz, J.W. Davis, M. Poon, R.G. Macaulay-Newcombe, *J. Nucl. Mater.* 258–263 (1998) 889.
- [10] T. Venhaus, R. Causey, R. Doerner, T. Abeln, *J. Nucl. Mater.* 290–293 (2001) 505.